World Journal of Radiology

Online Submissions: http://www.wjgnet.com/esps/
wjr@wjgnet.com
doi:10.4329/wjr.v4.i7.302

World J Radiol 2012 July 28; 4(7): 302-310
ISSN 1949-8470 (online)

ORIGINAL ARTICLE

Diffusion-weighted MRI in a liver protocol: Its role in focal lesion detection

Stefano Palmucci, Letizia Antonella Mauro, Martina Messina, Brunella Russo, Giovanni Failla, Pietro Milone, Massimiliano Berretta, Giovanni Carlo Ettorre

Stefano Palmucci, Letizia Antonella Mauro, Martina Messina, Brunella Russo, Giovanni Failla, Pietro Milone, Giovanni Carlo Ettorre, Radiodiagnostic and Oncological Radiotherapy Unit, University Hospital "Policlinico-Vittorio Emanuele", 95123 Catania, Italy

Massimiliano Berretta, Department of Medical Oncology, National Cancer Institute, 33081 Aviano (PN), Italy

Author contributions: Palmucci S, Messina M and Russo B planned the research, performed the study and analyzed the data; Ettorre GC approved the research; Milone P provided some magnetic resonance imaging studies; Palmucci S and Berretta M were involved in the collection of clinical data; Palmucci S and Failla G critically revised the data; Palmucci S wrote the paper, assisted by Russo B and Messina M; and Mauro LA corrected the manuscript.

Correspondence to: Stefano Palmucci, MD, Radiodiagnostic and Oncological Radiotherapy Unit, University Hospital "Policlinico-Vittorio Emanuele", 95123 Catania, Italy. spalmucci@sirm.org
Telephone: +39-95-3782360 Fax: +39-95-3782360

Received: September 8, 2011 Revised: February 21, 2012
Accepted: March 1, 2012
Published online: July 28, 2012

Abstract

AIM: To evaluate the role of diffusion-weighted imaging (DWI) in the detection of focal liver lesions (FLLs), using a conventional magnetic resonance imaging (MRI) protocol.

METHODS: Fifty-two patients (22 males, average age 55.6 years, range: 25-82 years), studied using a 1.5 Tesla magnetic resonance scanner, were retrospectively analyzed; detection of FLLs was evaluated by considering the number of lesions observed with the following sequences: (1) respiratory-triggered diffusion-weighted single-shot echo-planar (DW SS-EP) sequences; (2) fat-suppressed fast spin-echo (fs-FSE) T2 weighted sequences; (3) steady-state free precession (SSFP) images; and (4) dynamic triphasic gadolinium-enhanced images, acquired with three-dimensional fast spoiled gradient-echo (3D FSPGR). Two radiologists independently reviewed the images: they were blinded to their respective reports. DW SS-EP sequences were compared to fs-FSE, SSFP and dynamic gadolinium-enhanced acquisitions using a *t*-test. Pairs were compared for the detection of: (1) all FLLs; (2) benign FLLs; (3) malignant FLLs; (4) metastases; and (5) hepatocellular carcinoma (HCC).

RESULTS: Interobserver agreement was very good (weighted κ = 0.926, CI = 0.880-0.971); on the consensus reading, 277 FLLs were detected. In the comparison with fs-FSE, DW SS-EP sequences had a significantly higher score in the detection of all FLLs, benign FLLs, malignant FLLs and metastases; no statistical difference was observed in the detection of hepatocellular carcinoma (HCCs). In the comparison with SSFP sequences, DW SS-EP had significantly higher scores ($P < 0.05$) in the detection of all lesions, benign lesions, malignant lesions, metastases and HCC. All FLLs were better detected by dynamic 3D FSGR enhanced acquisition, with $P = 0.0023$ for reader 1 and $P = 0.0086$ for reader 2 in the comparison with DW SS-EP sequences; with reference to benign FLLs, DW SS-EP showed lower values than 3D FSPGR enhanced acquisition ($P < 0.05$). No statistical differences were observed in the detection of malignant lesions and metastases; considering HCCs, a very slight difference was reported by reader 1 ($P = 0.049$), whereas no difference was found by reader 2 ($P = 0.06$).

CONCLUSION: In lesion detection, DWI had higher scores than T2 sequences; considering malignant FLLs, no statistical difference was observed between DWI and dynamic gadolinium images.

Key words: Diffusion weighted magnetic resonance imaging; Liver; Liver disease; Magnetic resonance imaging

Peer reviewers: Roberto Miraglia, MD, Department of Diagnostic and Interventional Radiology, Mediterranean Institute for Transplantation and Advanced Specialized Therapies (IsMeTT), Via Tricomi 1, 90100 Palermo, Italy; Yasunori Minami, MD, PhD, Division of Gastroenterology and Hepatology, Department of Internal Medicine, 377-2 Ohno-higashi, Osaka-sayama, Osaka 589-8511, Japan; Yicheng Ni, MD, PhD, Professor, Biomedical Imaging, Interventional Therapy and Contrast Media Research, Department of Radiology, University Hospitals, KU Leuven, Herestraat 49, B-3000 Leuven, Belgium

Palmucci S, Mauro LA, Messina M, Russo B, Failla G, Milone P, Berretta M, Ettorre GC. Diffusion-weighted MRI in a liver protocol: Its role in focal lesion detection. *World J Radiol* 2012; 4(7): 302-310 Available from: URL: http://www.wjgnet.com/1949-8470/full/v4/i7/302.htm DOI: http://dx.doi.org/10.4329/wjr.v4.i7.302

INTRODUCTION

In the past twenty years, several magnetic resonance imaging (MRI) diagnostic techniques have gradually been introduced in the study of focal liver lesions (FLLs), increasing to the greatest possible extent the high contrast resolution inherent in the method. For instance, long echo-time T2 weighted sequences are widely used to characterize fluid-filled cystic lesions or hemangiomas; fat-containing lesions (adenomas, atypical focal nodular hyperplasia) can be diagnosed in cases of signal decay in out-of-phase T1-weighted spoiled gradient echo sequences[1]. More recently a gradual introduction of new hepato-specific agents - gadolinium-ethoxybenzyl-diethylenetriamine pentaacetic acid (Gd-EOB-DTPA, Primovist, Bayer Schering) and gadopentate dimeglumine (Gd-BOPTA, Multihance, Bracco Imaging) has significantly increased the diagnostic potential of MRI, especially in the preoperative management of patients with liver metastases[2,3]. In addition, three-dimensional gradient echo imaging allows a dynamic study of the liver, evaluating the behavior of FLLs in the arterial and portal phase after contrast administration[4]. In view of these considerations, non-invasive characterization of FLLs is a current diagnostic challenge.

The introduction of diffusion weighted imaging (DWI) in liver MRI fuelled high expectations with several encouraging studies[5-7]. High values of *b* - required for characterization - cannot be used to identify FLLs. It has been shown that the use of diffusion weighted single-shot echo-planar (DW SS-EP) sequences with a low *b*-value is important for the detection of hepatic lesions, especially for small-sized lesions. The acquisition of "black blood" images with DW SS-EP sequences makes it possible to easily differentiate vessels from focal small-sized lesions in the liver[8,9]. Parallel techniques reduce artifacts, such as "blurring" or magnetic susceptibility artifacts, increasing the signal-to-noise ratio (SNR)[10,11]; moreover, respiratory-triggered sequences offer a better possibility of SNR compared to breath-hold techniques[12]. Many studies have recently started to compare DWI to T1-weighted acquisition in the detection and characterization of liver lesions[13-15].

In diffusion imaging of the liver, the first difficulty concerns the choice of the appropriate *b*-value, which means the degree of weighting in diffusion. High b-values cannot be used because of the low SNR they determine: for these reasons, in this study we retrospectively evaluated the ability to detect lesions using relatively low *b*-value DWI (*b*-values extended from $b = 0\text{-}10$ to $b = 0\text{-}500$) in a routine liver MRI protocol. The characterization of FLLs was not considered in our work, because the role of DWI in this regard has already been widely debated in previous studies[5,15], and seems to be limited by overlapping[16].

In the detection of FLLs, diffusion weighted sequences were compared to fat suppressed fast spin-echo (fs-FSE) T2-weighted sequences, steady state free-precession (SSFP) sequences and dynamic triphasic gadolinium-enhanced acquisition, acquired with 3D fast spoiled gradient echo (FSPGR), emphasizing their advantages and limits.

MATERIALS AND METHODS

Patients and lesions

The study included 70 patients with a liver MRI study, performed on the basis of a clinical suspicion of FLL and/or for a morphological suspicion of FLL derived from a previous diagnostic exam (computed tomography or ultrasonography). In the revision analysis, the following exclusion criteria were adopted: (1) diffuse or "miliary" involvement of liver parenchyma (2 patients); (2) sequences with image quality damaged by artifacts, not included in the analysis (5 patients); and (3) incomplete liver MRI study (11 patients).

We retrospectively evaluated a total of 52 patients (22 males, 30 females, average age 55.6 years, range: 25-82 years), studied from November 2009 to February 2011. For detection and characterization of FLLs, the standard of reference in our study was based on: (1) the presence of previous diagnostic examinations and/or the follow-up; (2) the presence of the typical radiological pattern; and (3) the histopathology. On the consensus reading, 277 FLLs were detected: 135 of them were benign lesions, whereas 142 were malignant; the number of metastases and hepatocellular carcinomas (HCCs) observed were 114 and 28, respectively. Metastases were reported in 12 patients, whereas HCCs were found in 8 patients (Table 1).

The benign lesions detected were as follows: 44 hemangiomas were found in 14 patients, 77 cysts in 17 patients and 14 focal nodular hyperplasias (FNHs) in 9 patients (Table 1).

The diagnosis of cysts was made for hyperintense lesions in T2-weighted images, even with long echo-time, without any enhancement during contrast administration. The diagnosis of hemangioma was established as follows: (1) typical MRI findings of cavernous hemangiomas, represented by signal hyperintensity in T2-weighted images - even with long echo-time - and globular centripetal

Table 1 Patients and lesions

Total number of patients	52
Age (yr)	55.6
Gender	30 females, 22 males
FLLs distribution	
Patients with benign FLLs	35
Patients with hemangiomas	14
Patients with cysts	17
Patients with FNHs	9
Patients with malignant FLLs	20
Patients with metastases	12
Patients affected by breast cancer	1
Patients affected by colo-rectal cancer	9
Patients affected by melanoma	1
Patients affected by pancreatic cancrer	1
Patients with HCCs	8

Characteristics of the patients included in our study. The distribution of benign and malignant focal liver lesions (FLLs) among the patients is also reported, according to the different categories of lesions observed. HCC: Hepatocellular carcinoma.

enhancement during contrast administration[17,18]; and (2) typical behavior of capillary hemangiomas or high-flow related hemangiomas, with a hypervascular pattern on arterial phase and slight signal hyperintensity or isointensity in the delayed equilibrium phase[17,18]. In addition, the stability of lesion size was detected on serial cross-sectional imaging studies obtained from our archive or acquired with a mean follow-up of 8 mo.

The diagnosis of FNH was determined by histopathology in only one patient; the remaining FNHs were defined considering the following features: (1) a hypervascular aspect in MRI images during the arterial phase after contrast administration; (2) retention of hepato-specific contrast on delayed images (20 min after Gd-EOB-DTPA and 120 min after Gd-BOPTA); and (3) presence of a central scar, observed in cases of typical FNH. The uptake of hepato-specific contrast in the hepatobiliary phase and the absence of estrogen exposure were adopted as criteria to differentiate FNHs from adenomas. The diagnosis was also validated by the size stability of the lesions on serial cross-sectional imaging studies during follow-up (mean time of 9 mo and 24 d).

The diagnosis of HCC was determined by histopathology in 6 patients; in the remaining cases the presence of HCC was established on the basis of the typical imaging features (enhancement on the arterial phase, rapid wash-out and pseudocapsule on the delayed phase), according to clinical tests and a biomarker (increased serum levels of alpha-fetoprotein).

Metastatic malignant lesions were confirmed by biopsy in 6 patients; the remaining metastases were confirmed by diagnostic imaging features (target appearance for colic metastases) and by their enlarged size, which was evident after a mean follow-up time of 123.4 d (90 d was the shortest follow-up, 174 was the longest). The primary sites of metastases included breast carcinoma (n = 1), colorectal carcinoma (n = 9), melanoma (n = 1) and pancreatic carcinoma (n = 1).

Imaging protocol

The exams were performed using a 1.5 Tesla Magnetic Resonance (General Electric, Signa HDxt); an eight-channel phased-array coil was used for acquisition of liver images. Synchronization with patients' breath was achieved by placing a "respiratory" belt around their abdomen.

The study protocol included: (1) axial breath-hold FSPGR T1-weighted, with the following parameters: TR = 180 ms, TE = 2.2-4.4 ms (in and out of phase); flip angle 80; thickness = 6 mm; spacing = 1 mm; acquisition matrix = 256 × 224; number of averages = 1; acquisition type = 2D; (2) axial breath-hold SSFP - Fiesta - TR = 4.0 ms; TE = 1.7 ms; thickness = 6 mm; spacing = 1 mm; flip angle = 75; acquisition matrix = 256 × 224; number of averages = 1; acquisition type = 2D; and (3) axial breath-hold fs-FSE T2-weighted - spatial fat saturation; TR = 2100 ms; TE > 100 ms; thickness = 6 mm; spacing = 1 mm, flip angle = 90; acquisition matrix = 256 × 224; number of averages = 1; acquisition type = 2D.

DWI was acquired using a respiratory-triggered SS-EP technique with several b values (0-10/0-40/0-150/0-300/0-500); images obtained with b = 10 and b = 40 were also included in the evaluation and in the comparison with the other sequences.

Diffusion sequences were performed with the following parameters: TR = 1R-R, TE = 40 ms, EPI factor = 80, slice thickness = 6 mm, gap = 1 mm, flip angle = 90, acceleration factor = 2, FOV 32-44 cm, NSA = 2, acquisition time 39 s, half scan-factor = 2, band-width = 250 KHz, scan percentage = 100%, acquisition voxel = N/A, reconstruction voxel = N/A, acquisition matrix 192 × 160, reconstruction matrix = 256 × 256, spatial fat saturation = Yes - Water Excitation, isotropic motion gradient = SI, RL and AP with the Stejskal-Tanner Diffusion scheme.

All examinations included a dynamic multiphase 3D FSPGR T1-weighted sequence, acquired before and after a hepato-specific-gadolinium contrast agent (Gd-BOPTA 0.1 mmol/kg, Multihance 0.5 mol, Bracco Imaging, Italy or Gd-EOB-DTPA 25 μmol/kg - 0.1 mL/kg - Bayer Schering, Germany). Three-dimensional FSPGR sequences were acquired with the following parameters: TR = 4.2 ms; TE = 2.0 ms; thickness = 3 mm; flip angle = 12; acquisition matrix = 320 × 192; acquisition type = 3D. A dynamic multiphase hepatic acquisition (arterial, portal and delayed phases) was carried out using the smart prep system; when necessary, some studies were also completed with a delayed hepato-specific phase, acquired 20 min after Gd-EOB-DTPA, and 120 min after Gd-BOPTA administration. The contrast medium was administered by a MedRad double testis injector with a contrast injection rate of 2 mL/s for Gd-BOPTA and 1 mL/s for Gd-EOB-DTPA. In all patients an immediate bolus of physiological saline was injected after the contrast agent.

Detection of FLLs

Detection of FLLs was evaluated considering the number of liver lesions observed with different sequences: (1)

Table 2 Detection rate

	Tri-Gd T1	SSFP	fs-FSE	DWI	Consensus
All FLLs					277
Reader 1	266 (96)	161 (58)	187 (68)	234 (84)	
Reader 2	256 (92)	185 (67)	185 (67)	222 (80)	
Mean	261 (84)	186 (67)	186 (67)	228 (82)	
Benignant					135
Reader 1	134 (99)	89 (66)	89 (66)	116 (86)	
Reader 2	127 (94)	88 (65)	88 (65)	105 (78)	
Mean	130.5 (97)	88.5 (66)	88.5 (66)	110.5 (82)	
Malignant					142
Reader 1	132 (93)	99 (70)	99 (70)	118 (83)	
Reader 2	129 (91)	97 (68)	97 (68)	114 (80)	
Mean	130.5 (92)	98 (69)	98 (69)	116 (82)	
Metastases					114
Reader 1	104 (91)	82 (72)	82 (72)	100 (88)	
Reader 2	101 (89)	79 (69)	79 (69)	97 (85)	
Mean	102.5 (90)	80.5 (71)	80.5 (71)	98.5 (86)	
HCC					28
Reader 1	28 (100)	17 (60)	17 (60)	18 (64)	
Reader 2	28 (100)	18 (64)	18 (64)	17 (60)	
Mean	28 (100)	17.5 (62)	17.5 (62)	17.5 (62)	

Detection rate observed by triphasic gadolinium-enhanced T1 sequences (Tri-Gd T1), steady-state free precession (SSFP), fat-suppressed fast spin-echo (fs-FSE) and diffusion-weighted imaging (DWI) sequences. The values are divided according to the different categories of lesions analyzed in the study. HCC: Hepatocellular carcinoma; FLLs: Focal liver lesions.

respiratory-triggered DW SS-EP; (2) fs-FSE T2 weighted sequences with long TE (> 100 ms); (3) SSFP images; and (4) dynamic triphasic gadolinium-enhanced acquisition, acquired with multiphase 3D FSPGR T1-weighted sequences.

Location and size (maximum axial diameter) were reported for each lesion.

The measurements were carried out by two radiologists with more than two years of experience in body MRI. Radiologists reviewed images independently; sequences were randomized. The following pairs were compared in the number of FLLs detected: (1) DW SS-EP sequences *vs* fs-FSE; (2) DW SS-EP sequences *vs* SSFP; and (3) DW SS-EP sequences *vs* dynamic gadolinium-enhanced acquisition.

In the detection of lesions, these compared pairs were studied for: (1) all FLLs; (2) benign FLLs; (3) malignant FLLs; (4) metastases; and (5) HCC.

The number of FLLs was finally confirmed by viewing: (1) all sequences performed in the MR examination, including unenhanced T1 sequences, conventional T2 sequences, DWI sequences and enhanced 3D FSPGR acquisitions; when available, the hepato-specific phase was also considered to validate the number of lesions; and (2) previous or subsequent MR examinations; patient history was also considered to assess the number of lesions, in patients who underwent surgical intervention or biopsy.

Statistical analysis

A statistical analysis was performed using Win-Stat Software and a MedCalc program (MedCalc® version 11.4.4.0., MedCalc Software bvba). Interobserver agreement was evaluated for both radiologists involved in the detection analysis, by calculating the simple κ coefficient. The k-value was interpreted according to the following classification: < 0.20 poor; 0.20-0-40 fair; 0.41-0.60 moderate; 0.61-0.80 good; 0.81-1.00 very good. For the different classes of FLLs (all lesions, benign lesions, malignant lesions, metastases, HCCs) the detection rate was calculated as: the number of lesions observed/total number provided by consensus reading for each category. The number of lesions observed with conventional T2 sequences (fs-FSE), SSFP sequences, respiratory-triggered DW SS-EP sequences (acquired from b = 0-10 to b = 0-500 values) and 3D FSPGR post-gadolinium acquisitions were compared using a paired samples t-test.

RESULTS

Interobserver agreement was very good (weighted κ = 0.923, CI = 0.873-0.972). Detection rates for all FLLs, benign lesions, malignant lesions, metastases and HCC are shown in Table 2.

DW SS-EP sequences vs fs-FSE

DW SS-EP sequences showed a higher score when compared with conventional breath-hold T2-weighted sequence fs-FSE, with P = 0.001 for reader 1 and P = 0.0019 for reader 2 (Figure 1A). Considering benign FLLs (Figure 1B), DW SS-EP sequences showed higher values than fs-FSE sequences (P = 0.00 017 for reader 1 and P = 0.01 for reader 2) and SSFP sequences (P = 0.00 013 for reader 1 and P = 0.02 for reader 2); in the evaluation of malignant lesions (Figure 1C), DW SS-EP showed higher scores than fs-FSE only for reader 1 (P = 0.023), whereas no statistical difference was observed by reader 2 (P = 0.053). In the detection of metastases (Figure 1D), a significant statistical difference was observed for both readers, with P = 0.026 for both readers; no statistical difference was found in the detection of HCC (Figure 1E).

DW SS-EP sequences vs SSFP

With reference to all FLLs (Figure 1A), DW SS-EP sequences showed the highest score compared with SSFP sequences, with P = 0.001 for reader 1 and P = 0.00 035 for reader 2. The number of benign FLLs (Figure 1B) detected by DW SS-EP sequences was significantly higher, with P = 0.00 013 and P = 0.02 for reader 1 and reader 2, respectively.

DW SS-EP sequences also had higher scores in evaluating malignant lesions, metastases and HCC (Figure 1C-E), with significant P values (P < 0.05); in fact, the mean percentage of metastases detected by DW SS-EP was 86.4%, whereas the value observed using fs-FSE was 70%; also in the detection of HCCs, diffusion sequences were slightly superior to fs-FSE images.

DW SS-EP sequences vs dynamic 3D FSPGR gadolinium-enhanced acquisition

All FLLs were better detected by dynamic 3D FSPGR enhanced acquisition, with P = 0.0023 for reader 1 and P

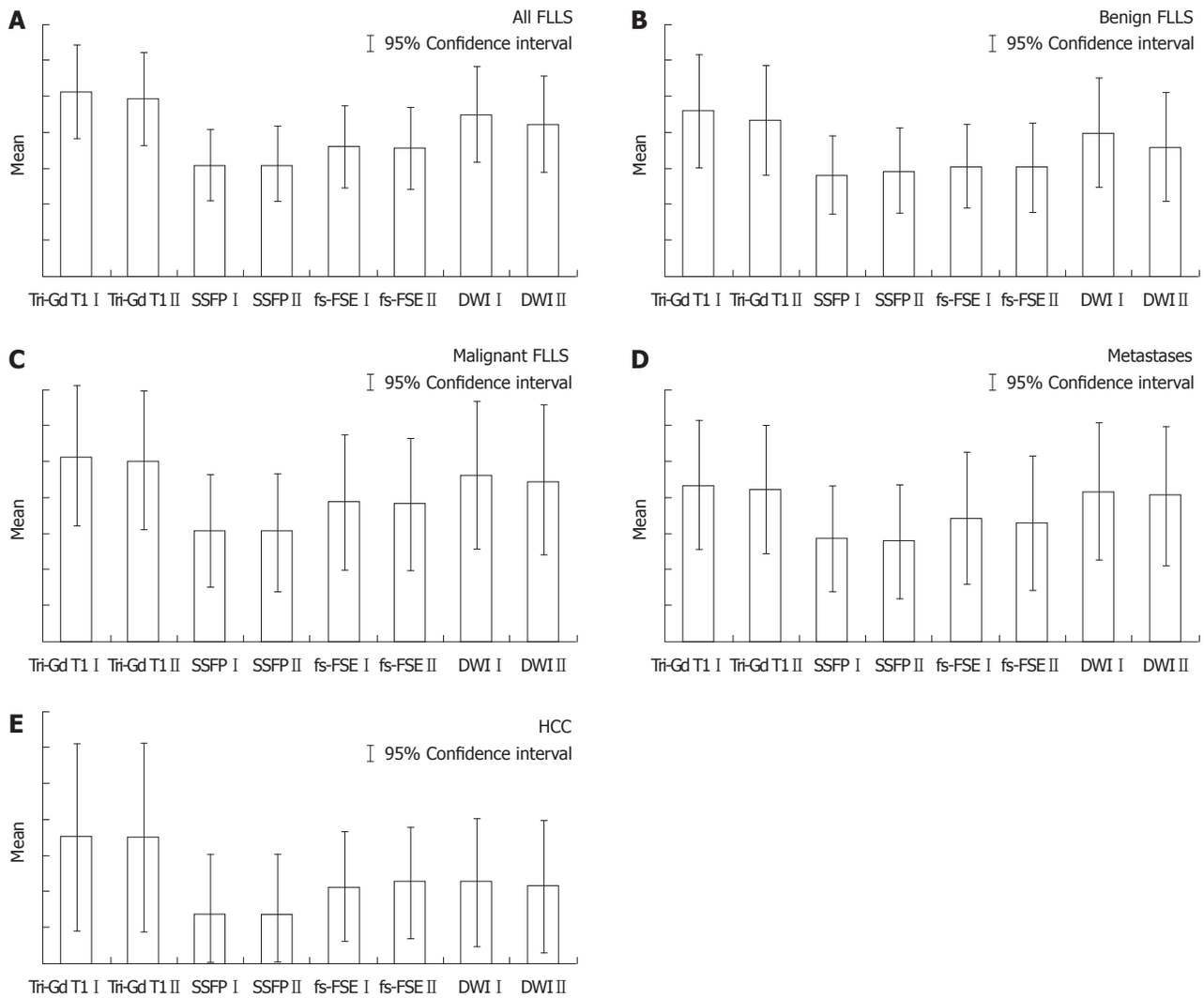

Figure 1 Histograms comparing the different sequences (A-E). Histograms showing the comparison between the mean values of lesions detected among different sequences, for the classes of focal liver lesions (FLLs) [all lesions, benign lesions, malignant lesions, metastases, hepatocellular carcinomas (HCCs)]. I = reader 1; II = reader 2; Tri-Gd T1: Triphasic gadolinium T1-weighted sequence; fs-FSE: Fat suppressed fast spin-echo sequence; SSFP: Steady state free precession; DWI: Diffusion weighted imaging.

= 0.0086 for reader 2 in the comparison with DW SS-EP sequences (Figure 1A).

In the detection of benign FLLs (Figure 1B), DW SS-EP had lower values than 3D FSPGR enhanced acquisition, with $P = 0.011$ and $P = 0.012$ (reader 1 and 2, respectively); in fact - with reference to the detection of benign lesions - reader 1 identified 116/135 of these lesions, whereas reader 2 had a lower score - 105/135; dynamic gadolinium-enhanced acquisitions identified 134 and 127 lesions (reader 1 and reader 2, respectively); mean detection rate was 81.8% for DWI and 96.6% for dynamic enhanced gadolinium T1 weighted FSPGR acquisition.

No statistical differences (Figure 1C-E) were observed by the readers in the detection of malignant lesions ($P = 0.09$ and $P = 0.07$). Detection rates of malignant lesions by diffusion sequences were 83% for reader 1 and 80% for reader 2, whereas enhanced gadolinium 3D FSPGR had higher values - 92.9% and 90.8%, respectively.

With regard to metastases, gadolinium-enhanced 3D FSPGR had a mean score of 102.5 for metastases identified, whereas DWI detected 98.5 metastatic lesions, with a detection rate of 89.9% and 86.4%, respectively; comparing the mean values of metastases observed through the paired samples *t*-test, no statistical difference was found ($P = 0.52$ and $P = 0.56$).

With regard to HCCs, a very slight difference was reported by reader 1 ($P = 0.049$), whereas no difference was found by reader 2 ($P = 0.06$); in our results, diffusion images allowed the identification of 17 and 18 lesions for reader 1 and for reader 2, respectively, with a mean detection rate of 17.5 lesions (62.5%), whereas all HCCs were correctly identified by 3D FSPGR images.

DISCUSSION

In recent years, some studies have emphasized the role of DWI in the characterization and detection of FLLs[5-7,9-12,19-21].

Furthermore, DWI could provide an additional tool in oncological patients, where a correct assessment of the number and localization of FLLs is essential in choosing suitable treatment. In fact, DWI provides better detection of FLLs than other T2-conventional sequences, and our results confirm what has recently been published in the literature. For instance, in a previous study by Bruegel *et al*[10], the sensitivity of DWI was higher than standard breath-hold and respiratory-triggered T2 weighted sequences in the diagnosis of 66 small hepatic metastatic lesions (sensitivity value of 0.85 and 0.26-0.44, respectively)[10]. In a study by Holzapfel *et al*[21], the detection of small FLLs seemed to be significantly increased by respiratory-triggered diffusion sequences, which produced better image quality because of high spatial resolution and an adequate SNR[22]. In the detection of metastases, when DWI was compared to fs-FSE sequences and to SSFP, we found a significantly higher number of lesions identified by both readers using DWI; the highest detection rate - shown by DWI in the detection of FLLs - was probably due to the 'black blood effect' of diffusion-weighted images: this property makes it easier to distinguish small FLLs from hepatic vessels, which may determine false-positive pseudolesions on T2-weighted turbo spin-echo images.

In view of its capability to detect FLLs, DWI has been widely introduced in liver imaging, and many studies have recently emphasized its additional values in liver imaging in order to detect malignant FLLs[13-15]. In this regard, a routine MRI protocol should ideally use all possible strategies, including many un-enhanced scans: in and out-of-phase T1-weighted sequences, T2-weighted FSE sequences - even with spatial fat saturation or different echo-time, white-blood sequences for morphologic assessment of liver anatomy such as steady-state sequences, and SSFSE sequences to emphasize T2-content; dynamic multiphase gadolinium-enhanced acquisitions are necessary to subsequently evaluate FLLs and to study their behavior in the arterial, portal and late phases. For this reason, the role of DWI in a liver MRI protocol should be assessed comparing the diffusion sequences not only to the conventional T2 sequences, but it must also include the dynamic enhanced gadolinium acquisitions.

In a study by Löwenthal *et al*[15] - considering only the detection of benign FLLs - a statistical difference in the comparison between DWI and hepatobiliary phase (MR-late) Gd-EOB-DTPA-enhanced images was reported; no difference was observed between DWI and dynamic (MR-dyn) Gd-EOB-DTPA-enhanced images, unlike the data reported in our comparison. This may be explained by the fact that DWI is less reliable than dynamic enhanced gadolinium FSPGR acquisitions, being much more sensitive to magnetic susceptibility artifacts. For instance, in our study, 6 cases of FNHs were missed by both readers evaluating only the diffusion-weighted images, probably due to their location in the parenchyma of the left lobe, near the gastric area: in this area DWI (Figure 2) could be affected by magnetic susceptibility or motion artifacts related to cardiac and gastric wall.

On analyzing the comparison using the *t*-test, no statistical difference between the number of lesions identified by DWI and dynamic enhanced gadolinium acquisition was observed, and DWI could be considered a valid diagnostic tool in the detection of malignant lesions in a liver study, even if they are characterized by a lower sensitivity in comparison to the dynamic acquisition. The high detection rate using DWI is especially observed in the evaluation of metastases, as confirmed in other studies[14]. The good results obtained using DWI in our study may be explained by the application of respiratory triggering, which produced better image quality because of high spatial resolution and an adequate SNR[12]; use of the respiratory-triggered modality in the diffusion images increases the spatial resolution, but requires a longer time for the acquisition. In addition, the use of low b-value diffusion sequences, acquired by parallel techniques, reduces artifacts such as "blurring" or magnetic susceptibility artifacts, increasing the SNR[10,11].

In a recent study by Kenis *et al*[13], DWI was used in the staging of oncological disease in patients with impaired renal function; in this study, MR showed a significant additional capability in the detection of metastases when considering DWI and gadolinium MRI together[13]. Kenis *et al*[13] analyzed three image sets: unenhanced T1 and T2 acquisitions/gadolinium-enhanced T1, DWI and a combination set; all observers reported high sensitivity values using the combination set of images; as a consequence, diagnostic accuracy increased significantly when DWI was added to Gd-MRI.

DWI is limited in the detection of HCC, with a mean detection rate (62.5%) lower than 3D FSPGR enhanced images (100%). Five HCC lesions missed by both readers were located in a subdiaphragmatic liver segment close to the heart or gastric wall (Figure 3): again, the lower diagnostic accuracy of DWI was probably related to the presence of magnetic susceptibility or motion artifacts in these locations, and even if the introduction of triggered-acquisition increased their image quality, we suggest that the evaluation of these areas could be limited. Similarly, magnetic susceptibility artifacts caused by colonic loop - often located very close to the caudal portion of the right liver - reduces imaging quality on diffusion images, with low signal intensity of parenchyma and loss of liver profile: one metastasis missed by both readers was located in the caudal portion of the IV segment, near to the colonic wall (Figure 4). In addition, lower scores obtained with DWI in our study - regarding the detection of HCCs - may also be explained by the different signal intensity observed in these lesions: in fact, in a recent study by Kim *et al*[14] they were isointense or hyperintense to the liver[14]. In a cirrhotic liver, HCCs may show the same signal intensity as the surrounding parenchyma, involved in a chronic fibrotic process, and as a consequence the detection and characterization of HCCs may be difficult[14].

Although some artifacts may affect the imaging quality of diffusion images, the highest detection rate observed in a liver MRI protocol suggest that they can easily help radiologists in the detection of FLLs, and in particular,

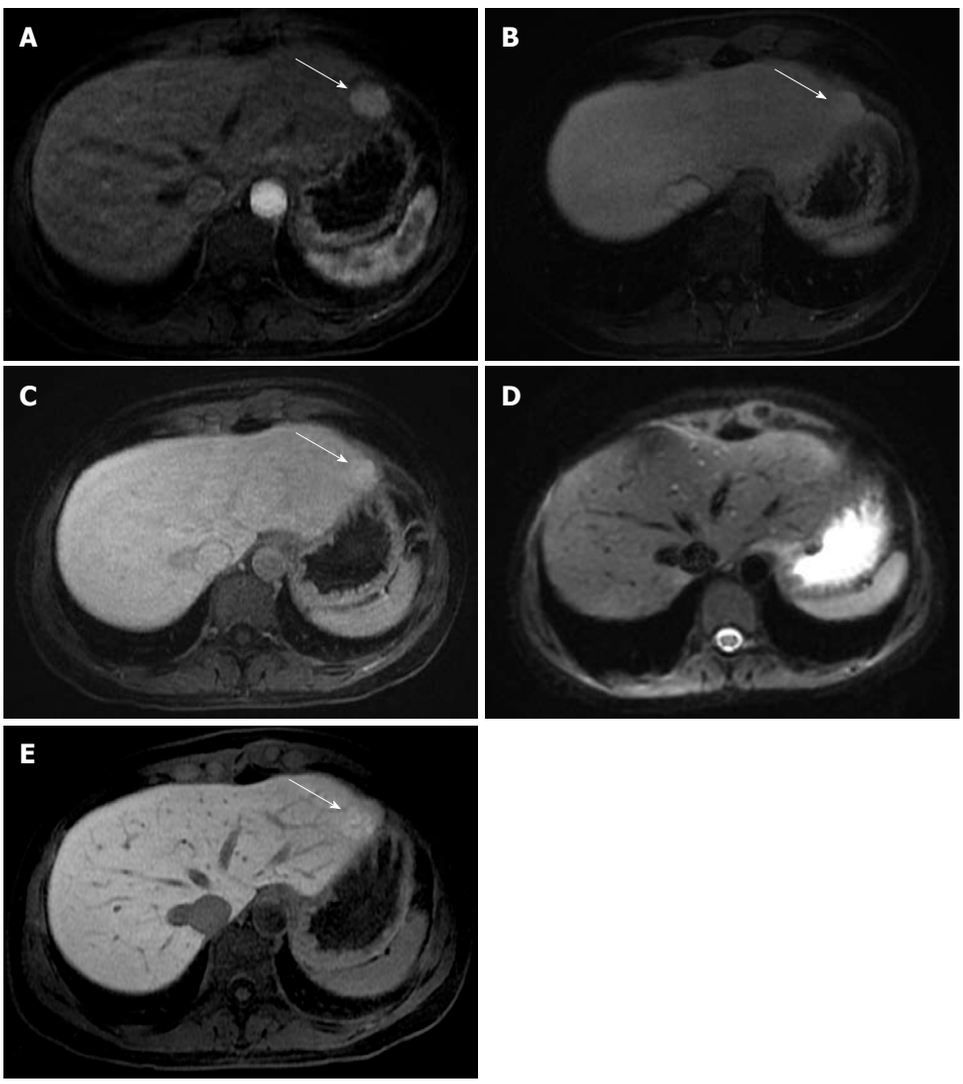

Figure 2 Focal nodular hyperplasia found in the left liver lobe. A: A round-shaped solid lesion (arrow) is depicted in the left liver lobe (in the Ⅱ segment); B, C: The lesion (arrow) appears homogeneously hyperintense in the arterial phase, and remains slightly hyperintense in the portal and in the equilibrium phase; D: The lesion was missed on the diffusion image by both readers, probably due to its location near the gastric wall, along the liver surface; E: In the hepato-specific phase, the lesion (arrow) shows uptake of gadolinium-ethoxybenzyl-diethylenetriamine pentaacetic acid; a diagnosis of focal nodular hyperplasia was suggested due to the dynamic behavior observed after contrast administration.

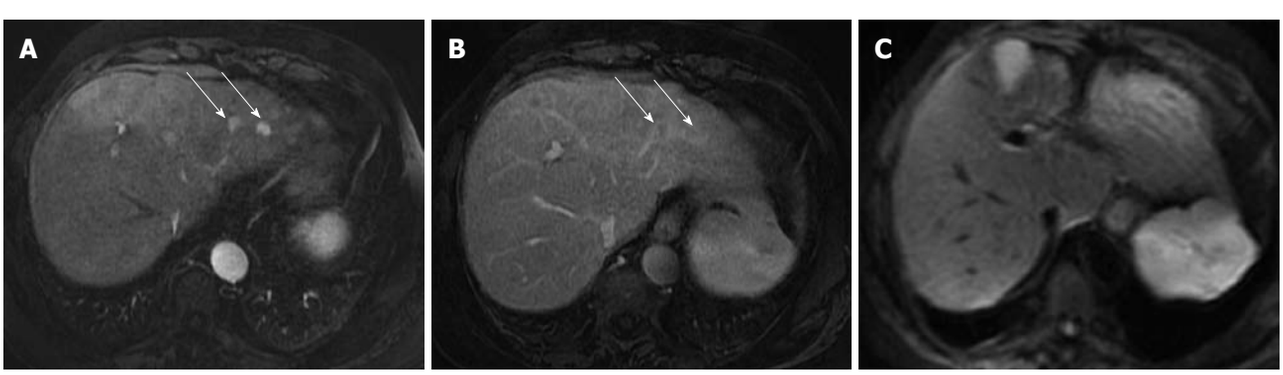

Figure 3 Hepatocellular carcinoma in the left liver lobe. A: Hypervascular lesions depicted (arrows) in the arterial phase; B: Lesions show wash-out in the venous phase (arrows), suggesting the diagnosis of hepatocellular carcinomas; C: On diffusion imaging, acquired at b10 value, lesions were not detected by the readers, due to their location near the gastric wall.

in the evaluation of metastases. These lesions are often reported with a larger size in the diffusion images, in comparison to the measurements observed by enhanced acquisitions. This larger size is better depicted in the

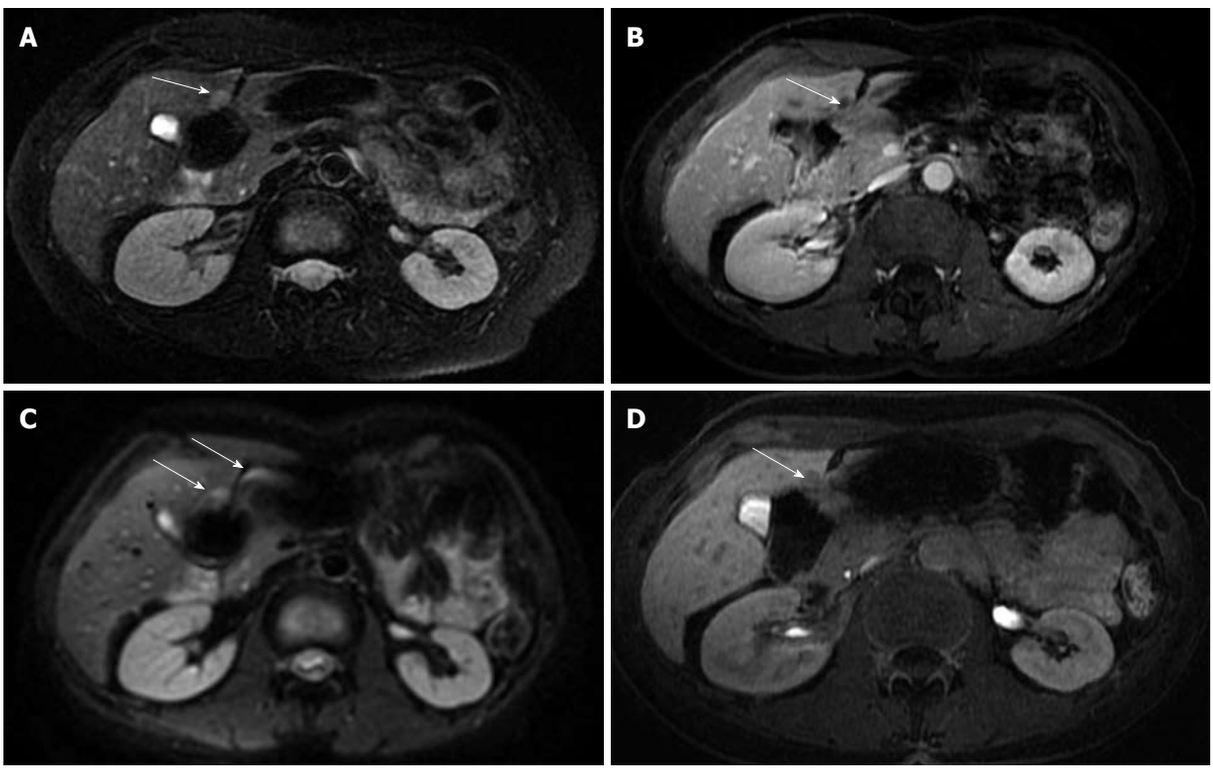

Figure 4 Metastasis in the Ⅳ segment. A: A metastatic lesion in colon carcinoma is depicted in the most caudal area of the Ⅳ liver segment, it was well depicted in the fat-suppressed fast spin-echo T2-weighted sequence (arrow); B: In the gadolinium-enhanced acquisition (arrow); C: The lesion is poorly represented in the diffusion-weighted imaging, covered by magnetic susceptibility artifacts due to the adjacent intestinal loop (arrows); D: Delayed imaging after gadolinium-ethoxybenzyl-diethylenetriamine pentaacetic acid confirmed the metastatic lesion (arrow).

follow-up of oncological patients, where lesions seem to be more reduced than those reported by gradient T1-weighted acquisition.

The main limitations of our work include the small number of histological proofs for FLLs: this may be explained by the fact that we retrospectively analyzed our study population and had many difficulties in collecting the patients' data. In addition, we discarded many exams when the image quality was damaged by artifacts, or in cases of incomplete liver MRI study.

There was no comparison between DW SS-EP and FSPGR images obtained in the hepato-specific phase; this may represent a limitation, considering the high potential value of liver-specific contrast assessed in the literature, especially in the evaluation of HCC[22]. Unfortunately, the number of exams including the hepato-specific phase in our study was not consistent and adequate for statistical analysis.

In conclusion, DWI may be very helpful to radiologists in a liver MRI protocol, increasing the detection of FLLs; considering the data reported in our study, the reliability of DWI is slightly lower than dynamic 3D FSPGR gadolinium-enhanced acquisition, but higher than conventional T2-weighted sequences. Regarding malignant FLLs, no statistical difference was found between DWI and conventional dynamic gadolinium images in our study; nevertheless, we feel contrast administration is mandatory to ensure the absence of malignant liver diseases, especially HCCs.

COMMENTS

Background

The introduction of diffusion weighted imaging (DWI) in liver magnetic resonance imaging (MRI) fuelled high expectations: **in the assessment of diffuse** and focal parenchymal disease, DWI is the latest added value in liver MRI.

Research frontiers

The use of diffusion weighted single-shot echo-planar (DW SS-EP) sequences with low *b*-value is important for the detection of hepatic lesions, especially for small-sized lesions. The acquisition of "black blood" images with DW SS-EP sequences makes it possible to easily differentiate vessels from focal small-sized lesions in the liver. In addition to the use of low *b*-value diffusion sequences, parallel techniques reduce artifacts, such as "blurring" or magnetic susceptibility artifacts, increasing the signal-to-noise ratio.

Innovations and breakthroughs

With regard to the detection all focal liver lesions (FLLs), in this study the authors retrospectively compared DWI with both T2-weighted conventional sequences and three dimensional dynamic gadolinium images. This study brings into focus the ability of DWI to detect FLLs when inserted in a complete standard liver MRI protocol.

Applications

The results suggest that DWI may be adopted as "a standard sequence" in a liver MRI protocol, owing its ability to detect FLLs.

Terminology

DWI is an imaging modality based on the measurement of the "free water" in biological tissues. Water molecules move randomly, in the so-called Brownian motion. Because of the different cellularity and percentage of free water, tissues may produce variable signal intensity, and DWI may help in detecting lesions.

Peer review

In this manuscript, the authors described the usefulness of diffusion-weighted imaging in detection of focal liver lesions. This topic is interesting; however, some revisions are needed to improve your manuscript.

REFERENCES

1 **Prasad SR**, Wang H, Rosas H, Menias CO, Narra VR, Middleton WD, Heiken JP. Fat-containing lesions of the liver: radiologic-pathologic correlation. *Radiographics* **2005; 25**: 321-331

2 **Zech CJ**, Herrmann KA, Reiser MF, Schoenberg SO. MR imaging in patients with suspected liver metastases: value of liver-specific contrast agent Gd-EOB-DTPA. *Magn Reson Med Sci* 2007; **6**: 43-52

3 **Bluemke DA**, Sahani D, Amendola M, Balzer T, Breuer J, Brown JJ, Casalino DD, Davis PL, Francis IR, Krinsky G, Lee FT, Lu D, Paulson EK, Schwartz LH, Siegelman ES, Small WC, Weber TM, Welber A, Shamsi K. Efficacy and safety of MR imaging with liver-specific contrast agent: U.S. multicenter phase III study. *Radiology* 2005; **237**: 89-98

4 **Elsayes KM**, Narra VR, Yin Y, Mukundan G, Lammle M, Brown JJ. Focal hepatic lesions: diagnostic value of enhancement pattern approach with contrast-enhanced 3D gradient-echo MR imaging. *Radiographics* **2005; 25**: 1299-1320

5 **Ichikawa T**, Haradome H, Hachiya J, Nitatori T, Araki T. Diffusion-weighted MR imaging with a single-shot echoplanar sequence: detection and characterization of focal hepatic lesions. *AJR Am J Roentgenol* 1998; **170**: 397-402

6 **Bruegel M**, Rummeny EJ. Hepatic metastases: use of diffusion-weighted echo-planar imaging. *Abdom Imaging* 2010; **35**: 454-461

7 **Taouli B**, Tolia AJ, Losada M, Babb JS, Chan ES, Bannan MA, Tobias H. Diffusion-weighted MRI for quantification of liver fibrosis: preliminary experience. *AJR Am J Roentgenol* 2007; **189**: 799-806

8 **Hussain SM**, De Becker J, Hop WC, Dwarkasing S, Wielopolski PA. Can a single-shot black-blood T2-weighted spin-echo echo-planar imaging sequence with sensitivity encoding replace the respiratory-triggered turbo spin-echo sequence for the liver? An optimization and feasibility study. *J Magn Reson Imaging* 2005; **21**: 219-229

9 **Coenegrachts K**, Delanote J, Ter Beek L, Haspeslagh M, Bipat S, Stoker J, Van Kerkhove F, Steyaert L, Rigauts H, Casselman JW. Improved focal liver lesion detection: comparison of single-shot diffusion-weighted echoplanar and single-shot T2 weighted turbo spin echo techniques. *Br J Radiol* 2007; **80**: 524-531

10 **Bruegel M**, Gaa J, Waldt S, Woertler K, Holzapfel K, Kiefer B, Rummeny EJ. Diagnosis of hepatic metastasis: comparison of respiration-triggered diffusion-weighted echo-planar MRI and five t2-weighted turbo spin-echo sequences. *AJR Am J Roentgenol* 2008; **191**: 1421-1429

11 **Yoshikawa T**, Kawamitsu H, Mitchell DG, Ohno Y, Ku Y, Seo Y, Fujii M, Sugimura K. ADC measurement of abdominal organs and lesions using parallel imaging technique. *AJR Am J Roentgenol* 2006; **187**: 1521-1530

12 **Colagrande S**, Carbone SF, Carusi LM, Cova M, Villari N. Magnetic resonance diffusion-weighted imaging: extraneurological applications. *Radiol Med* 2006; **111**: 392-419

13 **Kenis C**, Deckers F, De Foer B, Van Mieghem F, Van Laere S, Pouillon M. Diagnosis of liver metastases: can diffusion-weighted imaging (DWI) be used as a stand alone sequence? *Eur J Radiol* 2012; **81**: 1016-1023

14 **Kim YK**, Kim CS, Han YM, Lee YH. Detection of liver malignancy with gadoxetic acid-enhanced MRI: is addition of diffusion-weighted MRI beneficial? *Clin Radiol* 2011; **66**: 489-496

15 **Löwenthal D**, Zeile M, Lim WY, Wybranski C, Fischbach F, Wieners G, Pech M, Kropf S, Ricke J, Dudeck O. Detection and characterisation of focal liver lesions in colorectal carcinoma patients: comparison of diffusion-weighted and Gd-EOB-DTPA enhanced MR imaging. *Eur Radiol* 2011; **21**: 832-840

16 **Miller FH**, Hammond N, Siddiqi AJ, Shroff S, Khatri G, Wang Y, Merrick LB, Nikolaidis P. Utility of diffusion-weighted MRI in distinguishing benign and malignant hepatic lesions. *J Magn Reson Imaging* 2010; **32**: 138-147

17 **Horton KM**, Bluemke DA, Hruban RH, Soyer P, Fishman EK. CT and MR imaging of benign hepatic and biliary tumors. *Radiographics* **1999; 19**: 431-451

18 **Kandpal H**, Sharma R, Madhusudhan KS, Kapoor KS. Respiratory-triggered versus breath-hold diffusion-weighted MRI of liver lesions: comparison of image quality and apparent diffusion coefficient values. *AJR Am J Roentgenol* 2009; **192**: 915-922

19 **Coenegrachts K**, Delanote J, Ter Beek L, Haspeslagh M, Bipat S, Stoker J, Steyaert L, Rigauts H. Evaluation of true diffusion, perfusion factor, and apparent diffusion coefficient in non-necrotic liver metastases and uncomplicated liver hemangiomas using black-blood echo planar imaging. *Eur J Radiol* 2009; **69**: 131-138

20 **Parikh T**, Drew SJ, Lee VS, Wong S, Hecht EM, Babb JS, Taouli B. Focal liver lesion detection and characterization with diffusion-weighted MR imaging: comparison with standard breath-hold T2-weighted imaging. *Radiology* 2008; **246**: 812-822

21 **Holzapfel K**, Bruegel M, Eiber M, Ganter C, Schuster T, Heinrich P, Rummeny EJ, Gaa J. Characterization of small (≤10 mm) focal liver lesions: value of respiratory-triggered echo-planar diffusion-weighted MR imaging. *Eur J Radiol* 2010; **76**: 89-95

22 **Ni Y**, Marchal G, Yu J, Mühler A, Lukito G, Baert AL. Prolonged positive contrast enhancement with Gd-EOB-DTPA in experimental liver tumors: potential value in tissue characterization. *J Magn Reson Imaging* **1994; 4**: 355-363

S- Editor Cheng JX **L- Editor** Webster JR **E- Editor** Xiong L